AFRL-AFOSR-VA-TR-2024-0195

Fundamental Interaction Mechanisms of Roughness-Induced Flows with Surface Textures

David Goldstein
UNIVERSITY OF TEXAS AT AUSTIN
110 INNER CAMPUS DR
AUSTIN, TX, 78712
USA

03/22/2024
Final Technical Report

Air Force Research Laboratory
Air Force Office of Scientific Research
Arlington, Virginia 22203
Air Force Materiel Command

REPORT DOCUMENTATION PAGE

PLEASE DO NOT RETURN YOUR FORM TO THE ABOVE ORGANIZATION.

1. REPORT DATE	2. REPORT TYPE	3. DATES COVERED	
20240322	Final	START DATE 20190501	END DATE 20231130

4. TITLE AND SUBTITLE
Fundamental Interaction Mechanisms of Roughness-Induced Flows with Surface Textures

5a. CONTRACT NUMBER	5b. GRANT NUMBER	5c. PROGRAM ELEMENT NUMBER
	FA9550-19-1-0145	61102F
5d. PROJECT NUMBER	**5e. TASK NUMBER**	**5f. WORK UNIT NUMBER**

6. AUTHOR(S)
David Goldstein

7. PERFORMING ORGANIZATION NAME(S) AND ADDRESS(ES)
UNIVERSITY OF TEXAS AT AUSTIN
110 INNER CAMPUS DR
AUSTIN, TX 78712
USA

8. PERFORMING ORGANIZATION REPORT NUMBER

9. SPONSORING/MONITORING AGENCY NAME(S) AND ADDRESS(ES)	10. SPONSOR/MONITOR'S ACRONYM(S)	11. SPONSOR/MONITOR'S REPORT NUMBER(S)
Air Force Office of Scientific Research 875 N. Randolph St. Room 3112 Arlington, VA 22203	AFRL/AFOSR RTA1	AFRL-AFOSR-VA-TR-2024-0195

12. DISTRIBUTION/AVAILABILITY STATEMENT
A Distribution Unlimited: PB Public Release

13. SUPPLEMENTARY NOTES

14. ABSTRACT
We report on the specific objectives of the grant which were to use a combination of immersed boundary DNS (at UT) and matched experiments at the KSWT (at TAMU) to (I) obtain a generalized understanding and development of simple models for interaction of vortices with control strips, (II) analyze of the effect of pressure gradients on roughness-induced transition (RIT) mechanisms and evaluate shielding effectiveness over realistic geometries and at high Reynolds numbers and (III) quantify interactions between perturbations introduced by different discrete roughness elements. (IV) The work also examined the generality of RIT mechanisms to other modes of (bypass) transition.

15. SUBJECT TERMS

16. SECURITY CLASSIFICATION OF:			17. LIMITATION OF ABSTRACT	18. NUMBER OF PAGES
a. REPORT U	b. ABSTRACT U	c. THIS PAGE U	UU	15

19a. NAME OF RESPONSIBLE PERSON	19b. PHONE NUMBER *(Include area code)*
GREGG ABATE	425-1779

Standard Form 298 (Rev.5/2020)
Prescribed by ANSI Std. Z39.18

Award Number: FA9550-19-1-0145

Report Type: Final

Reporting Periods: 05/01/2019-11/30/2023

Distribution Statement: I think it is ok for public release.

Program Officer Name: Dr. Gregg Abate

Project Title: Fundamental Interaction Mechanisms of
Roughness-Induced Flows with Surface Textures

Abstract: We report on the specific objectives of the grant which were to use a combination of immersed boundary DNS (at UT) and matched experiments at the KSWT (at TAMU) to (I) obtain a generalized understanding and development of simple models for interaction of vortices with control strips, (II) analyze of the effect of pressure gradients on roughness-induced transition (RIT) mechanisms and evaluate shielding effectiveness over realistic geometries and at high Reynolds numbers and (III) quantify interactions between perturbations introduced by different discrete roughness elements. (IV) The work also examined the generality of RIT mechanisms to other modes of (bypass) transition.

Final Report: Fundamental Interaction Mechanisms of Roughness-Induced Flows with Surface Textures

Award #FA9550-19-1-0145

PI David Goldstein (david@oden.utexas.edu), The University of Texas at Austin, TX 78712
co-PI Edward White (ebw@tamu.edu), Texas A&M University, TX77843 and
co-PI Sai Suryanarayanan (ssuryanarayanan@uakron.edu), University of Akron, OH 44325.

Program Officer: Dr. Gregg Abate

BACKGROUND

Mitigation of roughness induced transition (RIT) on aircraft wing leading edges is a fundamental fluid dynamical problem that is of interest to the Air Force**.** Our previous work (*Phys. Fluids* 31, 024101 (2019), *AIAA J.* (2020), sponsored by Award #FA9550-15-1-0345) studied RIT mechanisms, and demonstrated successful RIT mitigation in a zero pressure gradient (ZPG) flat plate boundary layer by shielding large discrete roughness elements (DREs) with distributed roughness patches or span oriented control strips in both direct numerical simulations (DNS) and experiments. It was found that there are four distinct stages in RIT, and the different mechanisms were understood from vorticity dynamics and linear stability theory points of view. While the upstream control strips reduced all components of the vortical disturbance generated at the DRE, the downstream strips specifically disrupted the streamwise vortices. As a result, the transient growth of wall normal vorticity by lift-up was reduced in both cases leading to transition mitigation. In order to further advance the technological implementation of roughness shielding strategies, we proposed a fundamental study of the interaction of vortices and other roughness induced perturbations with surface textures such as control strips, including in situations with imposed pressure gradients.

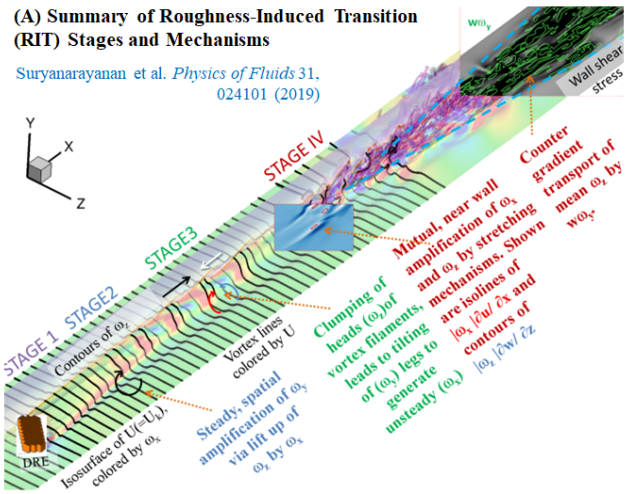

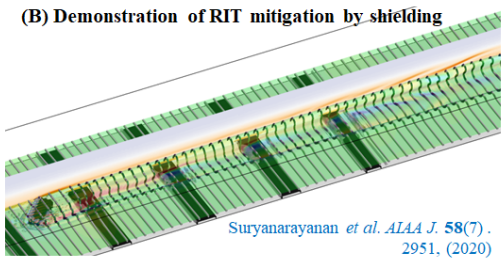

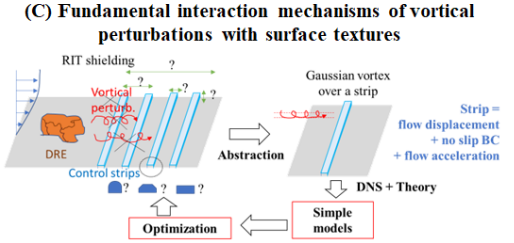

Figure 1. Summary of RIT mechanisms and shielding

PROPOSAL OBJECTIVES

Specific objectives of the current grant (Award #FA9550-19-1-0145) are to use a combination of immersed boundary DNS (UT) and matched experiments at the KSWT (TAMU) to (I) obtain a generalized understanding and development of simple models for interaction of vortices with control strips, (II) analyze of the effect of pressure gradients on RIT mechanisms and evaluate shielding effectiveness over realistic geometries and at higher Reynolds numbers and (III) quantify interactions between perturbations introduced by different DREs. (IV) The proposed work also examines the generality of RIT mechanisms to other modes of (bypass) transition.

SUMMARY OF RESULTS

(I) Generalized understanding and development of simple models for interaction of vortices with control strips

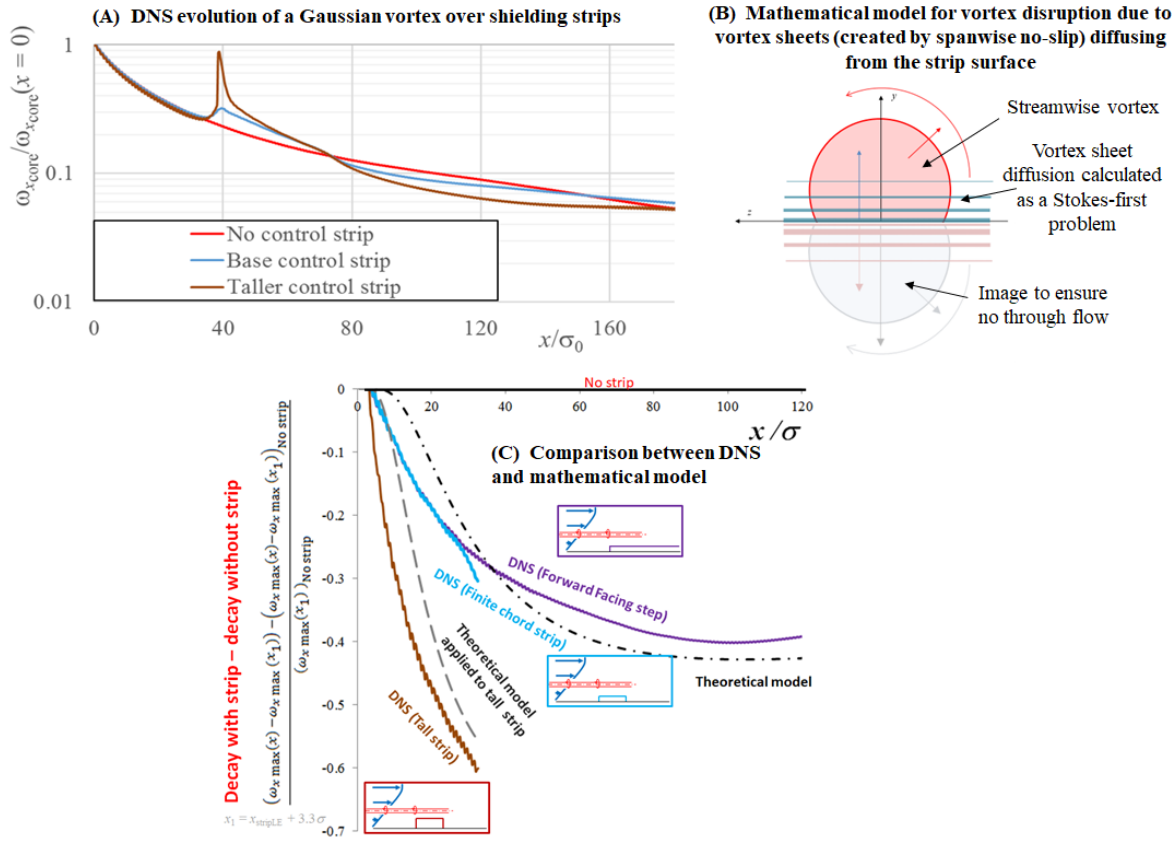

Figure 2. Interaction of streamwise vortices with strips - DNS and mathematical model

Our earlier work had shown that a downstream strip mitigates RIT by enhancing the dissipation of streamwise vortices. In the first year of this grant, we developed simple, analytical models to predict this enhanced dissipation given the strength and location of the vortex, downstream of the strip leading edge. Direct numerical simulations of a Gaussian streamwise vortex over a wall were performed to better understand and model the interaction of vortices with solid surfaces for optimization of RIT control by shielding. The evolution of the vortex over a slip wall is described by a diffusing vortex and

image model - an extension of the modified Oseen theory (Galilean transformation of the temporally evolving Oseen vortex). The addition of the no-slip boundary condition in z, creates an opposite signed ω_x at the wall that enhances the dissipation of the vortex. This effect can be satisfactorily modeled by superimposing the evolution of the vortex sheet (as in the Stokes first problem) with that of the diffusing vortex. The effect of spanwise strips in accelerating the dissipation of the streamwise vortex shown to be consistent with that observed in RIT simulations. Figure 2 compares the enhanced dissipation of a vortex over a shielding strip predicted by the theory with the DNS.

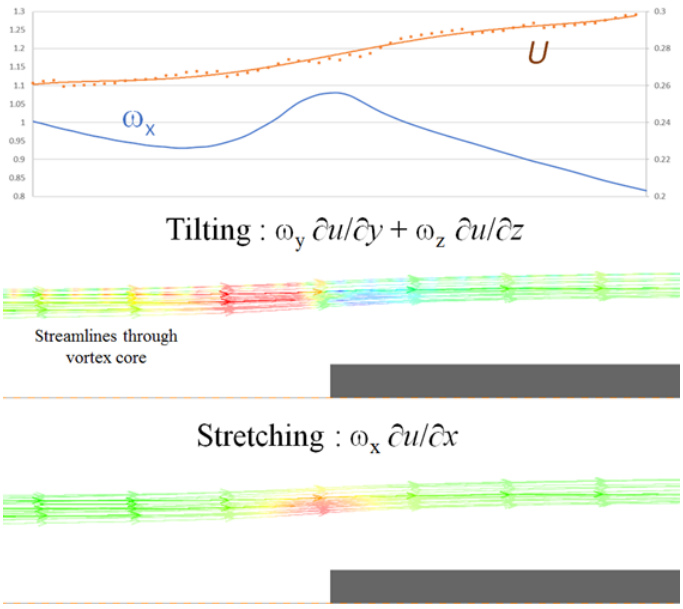

Figure 3. Flow acceleration and vortex intensification at the strip leading edge.

We next studied the vortex evolution over the strip leading edge to make the model self-contained and useful for control strip design. DNS results (Fig. 3) show that the vortex intensifies by both stretching and tilting mechanisms at the strip leading edge, though there is an eventual reduction in the vortex strength due to the enhanced dissipation over the strip surface. It is expected that these insights will be applied to further develop a complete predictive model for the evolution of vortices over shielding strips. These results were presented in AIAA Aviation 2020, APS DFD 2020 and AIAA Scitech 2022.

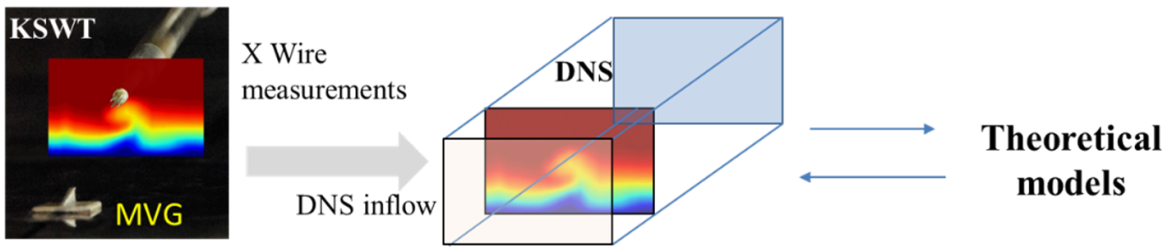

Figure 4. Philosophy of physio-cyber simulations of a streamwise vortex evolution downstream of a MVG.

To further our understanding of vortex-strip interactions, we conducted a wind-tunnel test campaign to measure the streamwise and spanwise velocities of stationary, streamwise-oriented vortices generated by microvortex generators (MVGs) with and without a shielding strip located a short distance

downstream of the MVG. These measurements were performed in the TAMU KSWT on a zero-pressure-gradient flat plate boundary layer using a unique two-wire hotwire anemometer probe that included the two wires in a V arrangement. This enables measurements of steady streamwise and spanwise velocities in close proximity to the surface of the flat plate. These measurements are used as an input into the DNS which generates the vertical velocity and streamwise vorticity (by enforcing continuity), and the matched experiments and simulations (as described in Fig. 4) provide insight on the fundamental interaction mechanisms.

Our current findings are:

1. The presence of a shielding strip meaningfully reduces spanwise velocities (a marker for streamwise vorticity) generated by a MVG. This results in reduced streamwise streak amplitude and can result in elimination of a turbulent wedge.
2. Using a rigid forcing in the physio-cyber hybrid approach to generate the experimentally measured w leads to unrealistic *v*, so using a weaker forcing appears to be the more appropriate way to generate an experimentally measured inflow condition.
3. The DNS with just *u* and *w* at the inflow (on the "cyber" side of the hybrid) satisfactorily appears to generate the correct *v* as demonstrated for cases where *v* is also known (like a Gaussian vortex).
4. The DNS of the Gaussian vortex and the theory provide reasonable agreement on peak values of *w* observed in the experiment.

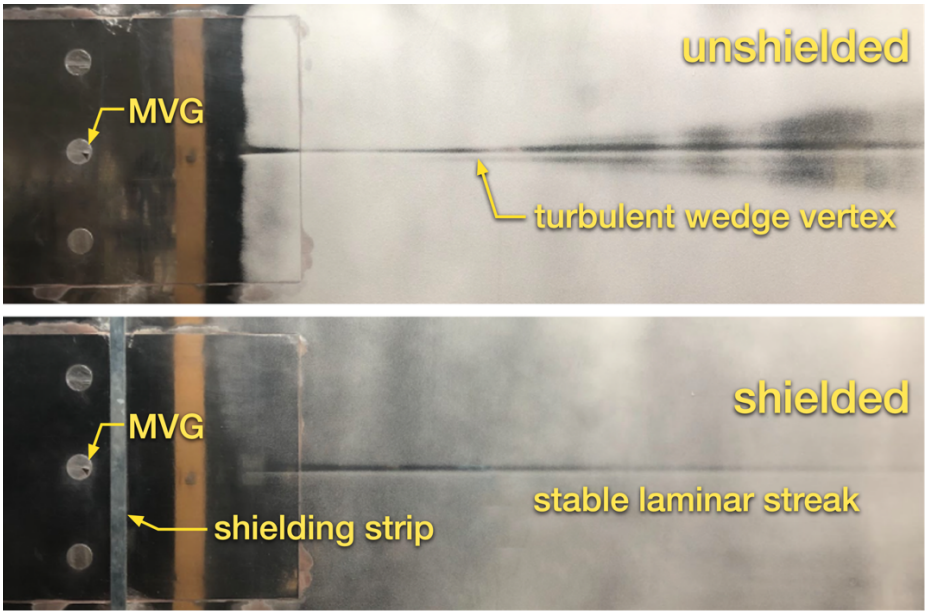

Figure 5. Naphthalene shear stress visualization of an unshielded (above) and shielded MVG wake. Application of the shielding strip downstream of the MVG eliminates the turbulent wedge.

The wind tunnel tests included extensive measurements at a nominal unit Reynolds number of Re'=500×10^3/meter on a zero-pressure gradient flat plate in the TAMU Klebanoff-Saric Wind Tunnel. In this facility, that Re' value corresponds to a freestream speed of approximately 7 m/s and a 7-mm-thick boundary layer (δ_{99}) at the MVG location 944 mm downstream of the flat-plate leading edge. This operating condition was selected because it produces a relatively thick boundary layer that permits V-wire measurements in close proximity to the surface (about 0.25 mm) with respect to the boundary-

layer thickness while also being a sufficiently fast freestream velocity to provide good wind-tunnel speed control and relatively low measurement uncertainty.

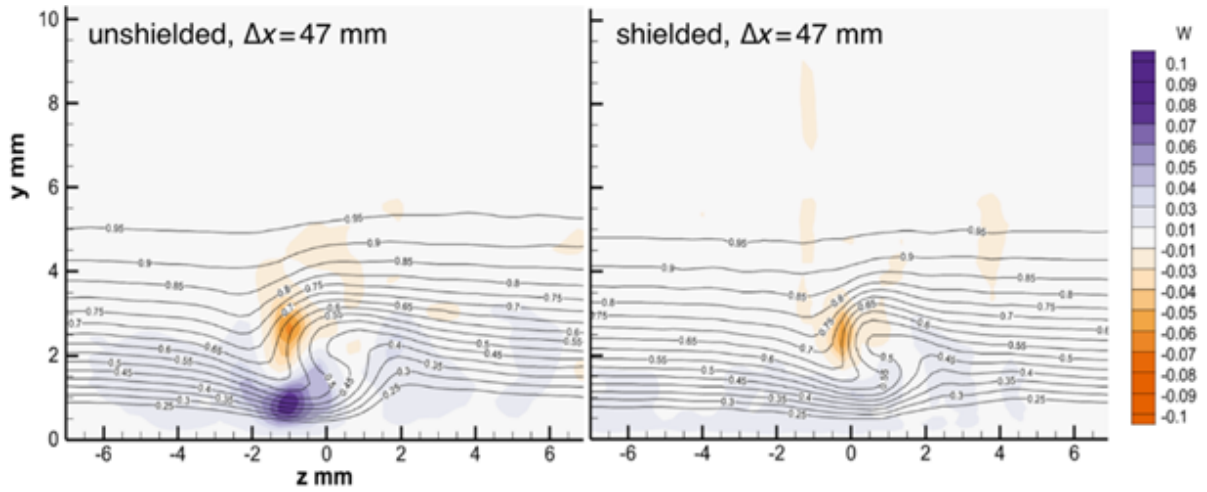

Figure 6. V-wire measurements demonstrate the effect of shielding strips on reducing the spanwise *W* velocity a marker for streamwise vorticity, color contours) and the amplitude of the streamwise streak (i.e., the *U′* velocity disturbance). Streamwise velocity *U* isolines are shown as black lines. Reducing the magnitude of *U′* stabilizes the shear layer near the top of the streak and prevents transition to turbulence.

The MVG used to create a streamwise vortex was 3-mm-tall, 6-mm-long and triangular in shape. Its inclination angle relative to horizontal was adjusted until it produced a turbulent wedge with a vertex in the middle of the test domain as shown in the top photograph of Fig. 5. A 1.2-mm-tall, 12-mm-wide shielding strip was attached to the plate with its leading edge located 19 mm downstream of the trailing edge of the MVG. With the strip in place, naphthalene flow visualization (bottom of Fig. 5) shows that the shielding strip successfully eliminates the turbulent wedge.

Extensive measurements of steady streamwise *U* and spanwise *W* velocities were made downstream of the MVG with and without a shielding strip present. These measurements used the V-wire technique developed as part of this work. Multiple data planes at different streamwise x positions were obtained upstream of, on top of, and downstream of the shielding strip. Measurements such as Fig. 6 confirm earlier DNS findings that the presence of the shielding strip reduces streamwise vorticity and the result is a reduction in the streamwise disturbance amplitude. Figure 6 shows data obtained 47 mm downstream of the MVG, 16 mm downstream of the trailing edge of the shielding strip. The contour colors indicate substantially reduced spanwise velocity as well as substantially less streamwise velocity disturbance. The reduction in streamwise velocity disturbance weakens the shear layer at the top of the overturning region. The weaker shear is less unstable to high-frequency fluctuations and transition to turbulence does not result in for the shielded configuration.

The downstream shielding concept relies on reducing streamwise vorticity, $\omega_x = \partial W/\partial y - \partial V/\partial z$. The V-wire approach cannot measure the wall-normal *V* velocity, only the spanwise *W* velocity. Therefore, the experiments use the magnitude of *W* only a as a marker for streamwise vorticity, not the vorticity itself. The limitation on the experimental data is overcome in this project by using the experimental measurements of *U* and *W* in a plane upstream of the shielding strip as inflow DNS data as described above. Then, the DNS is able to provide all of the flow-field data, *U*, *V* and *W* that are not all experimentally measurable.

(II) Effect of pressure gradients on RIT mechanisms and evaluation of control strategies on realistic geometries

The effect of pressure gradients on different RIT stages and mechanisms were studied using a vorticity dynamics point of view. Flow acceleration was imposed on specific streamwise extents of the flow in the DNS, and an analog of a setup shown in Fig. 7A was created using immersed boundary forces. The results suggest that both lift-up and subsequent amplification of the unsteady perturbations are mitigated by flow acceleration, though the mechanisms remained broadly similar as the ZPG case. The effect on lift-up is explained by the compression (negative stretching) of the wall-normal vorticity by negative dv/dy (Fig. 7B). Favorable pressure gradients (FPG) reduce turbulent wedge spreading and are shown to nearly arrest the spreading (see Fig. 7C) when sufficiently strong. FPG disrupts the wedge spreading cycle and inhibits the generation of ω_x 'pancakes' by the tilting of ω_z. These results have been presented at *TSFP11* and have been published in the *Intl. J. Heat and Fluid Flow*.

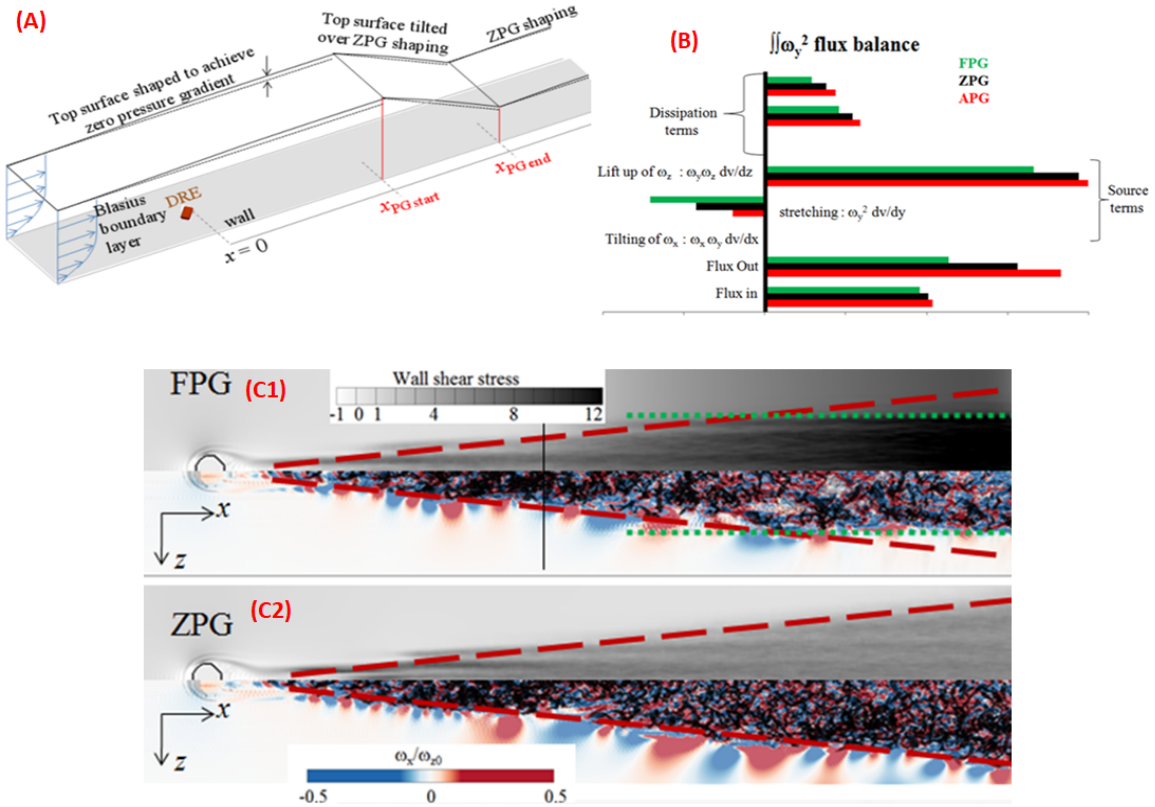

Figure 7. A. Illustration of the physical setup (shown here for FPG) the DNS aims to simulate. **B.** Effect of pressure gradients applied in RIT Stage II (lift-up) in altering different terms of the ω_y^2 flux balance. **C.** Effect of strong pressure gradients (in case C1) in affecting the evolution of a turbulent wedge (RIT stage IV)

Shielding effectiveness in a realistic and operationally relevant airfoil was tested in the TAMU Low-Speed Wind Tunnel (LSWT) using a 7-ft-span, 30-inch-chord 63(3)-418 airfoil operating near its design lift coefficient and up to $Re_c = 3.4\times10^6$. The experiment consisted of infrared (IR) thermography observations of turbulent wedges or their absence downstream of 3-mm-long, 1-mm-wide rectangular DREs oriented 45° from the streamwise direction. Figure 8A shows an example IR image. These were

located at s/c = 7.4% where environmental roughness would accumulate, in the strongly favorable pressure gradient region. Without shielding, these elements were found to have a critical roughness-based Reynolds number $Re_{kk,\mathrm{crit}}$ = 186±18 when the airfoil was at α=0° and 166±13 at α=2°. The lower $Re_{kk,\mathrm{crit}}$ at α=2° is attributable to the slightly less favorable pressure gradient at the DRE location at that angle of attack as compared to α=0°.

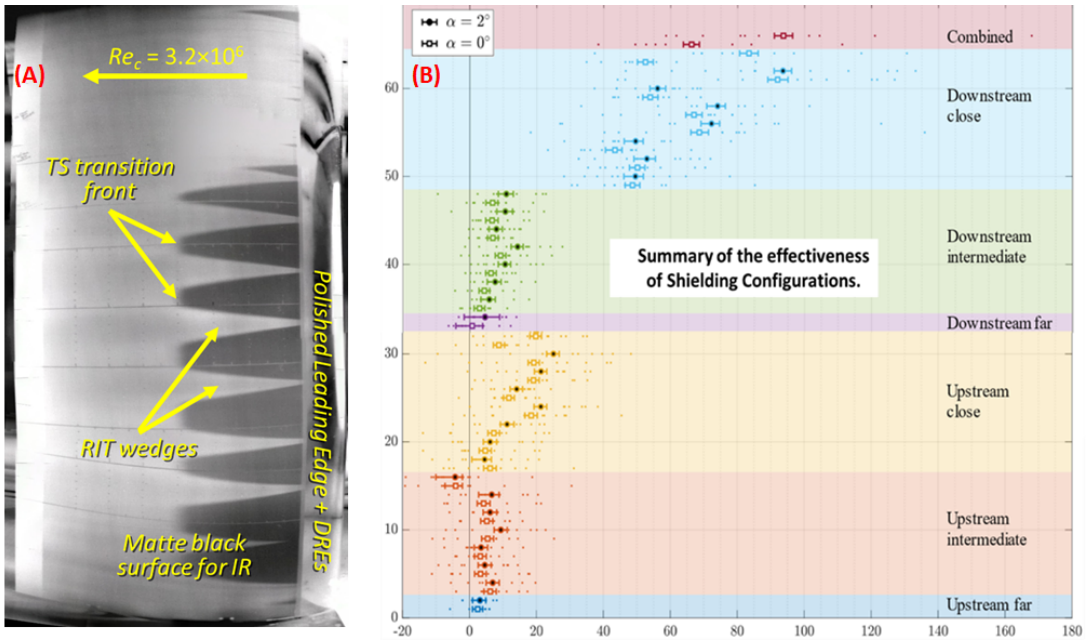

Figure 8. A. IR image showing turbulent wedges downstream of the DREs, flow is from the right. **B.** Summary of the effectiveness of shielding configurations

The unshielded $Re_{kk,\mathrm{crit}}$ values for the DREs are referred to as $Re_{kk,\mathrm{crit,baseline}}$. Once these values were established, a variety of upstream, downstream, and combined upstream and downstream shielding strips were applied and $Re_{kk,\mathrm{crit}}$ values were measured in the presence of those shielding treatments. The data is summarized as *shielding effectiveness*, $\eta = (Re_{kk,\mathrm{crit}} - Re_{kk,\mathrm{crit,baseline}})/Re_{kk,\mathrm{crit,baseline}}$, expressed as a percent value. A summary of these results is shown in Fig. 8B. No significant adverse effects of the shielding strips were observed so long as the shielding strips remained subcritical as there was no noticeable change in transition location due to TS waves.

Overall, both upstream and downstream shielding strips proved effective, especially when placed in close proximity to the DREs. Downstream shielding strips were somewhat more effective than upstream shielding strips. The best performance was observed for downstream shielding strips in very close proximity to the DREs. In some instances, $\eta > 60\%$ was achieved. Comparing the two angle of attack, marginally better shielding performance was observed for α = 2° as compared to α = 0°. This suggests improved performance effectiveness when the favorable pressure gradient is weaker. The design space exploration allowed for the identification of best-performing upstream and downstream shielding strip widths and thicknesses. The best-performing strip thickness-to-DRE height ratio was 0.51, and the best-performing strip-width-to-DRE-thickness ratio was 35. The simultaneous combination of upstream and downstream shielding proved to be more effective than either approach used individually. Shielding effectiveness was found to be similarly sensitive to strip thickness in the combined cases compared to the single shielding cases. In addition, the combined shielding runs provided an opportunity to evaluate the repeatability of four single shielding configurations. These

results were presented at the 2023 AIAA Aviation forum and are currently under consideration for publication in *AIAA Journal*.

The most effective approach for single-strip shielding was found to be downstream shielding with the shielding strip touching or nearly touching the downstream corner of the DRE. This effectiveness is likely due to the inhibition of a separation bubble by the strip. This hypothesis is experimentally supported in the final sequence of wind tunnel runs and by DNS. The experiments could not directly confirm this mechanism but DNS results shown in Fig. 9 support exactly the hypothesis that a separation bubble is suppressed by a close-proximity shielding strip and this effectively mitigates transition.

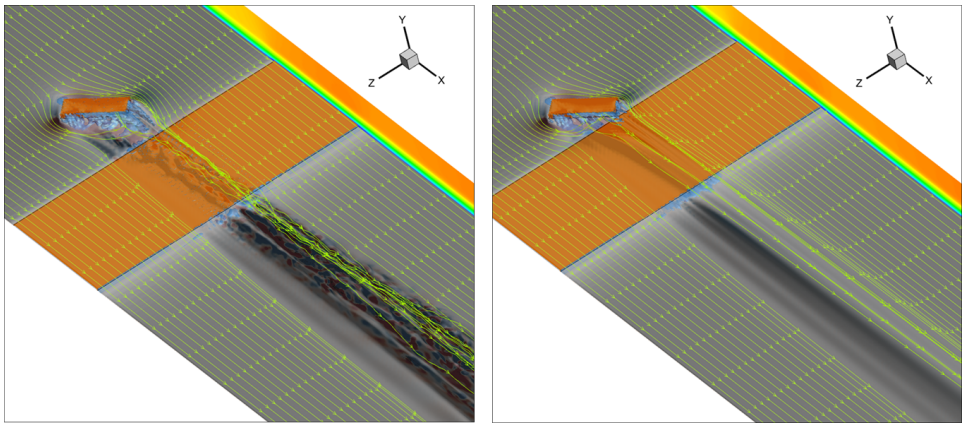

Figure 9. DNS with inflow profiles and pressure gradients matched with the LSWT airfoil experiments at Re_{kk} = 279 showing the effect of close shielding on the separation bubble behind the DRE**.**

(III) Interactions between perturbations introduced by different DREs

The mechanisms of boundary layer transition caused by multiple discrete roughness elements, as well as by a distributed roughness patch, were studied using our immersed boundary direct numerical simulations. The objective was to obtain a broad understanding of how discrete roughness elements can affect the flow around and downstream of neighboring roughness elements, with the aim of extending our mechanistic understanding and mitigation strategies for isolated-roughness-induced transition to a dense array of discrete roughness elements, and possibly distributed roughness. The results were analyzed from instability and vorticity points of view.

Results on the interactions of two DREs are shown in Fig. 10. It can be observed from Figure 10C that a tall DRE can cause an otherwise subcritical DRE nearby to transition. This is because of two main reasons: The proximity between the DREs affects the overall flow field, which can change the "receptivity" of the shorter DRE. This can be better observed in Fig. 10D which has two identical shorter DREs; the strength of the streamwise vortices behind the two are different. The second reason is that the secondary modal instability of the taller DRE disturbs the wake of the smaller DRE (which would have been stable if the background was quiet). This is best observed in Fig. 10F in which the DREs are staggered such that there is not a significant effect on *the receptivity* by DRE1 upon DRE2. The transitioning DRE can excite either the clumping mode or the swaying mode of the subcritical DRE; that is, the turbulent wedge of one DRE shakes the neighboring laminar wake until it too becomes unstable. The latter appears to be likely when the subcritical wake is forced by the disturbances at the edge of a nearby turbulent wedge (as seen in Fig. 10F). These results are particularly significant in real-

world situations such as an aircraft wing leading edge subject to insect splatter; a single large roughness could potentially cause the flow downstream of many smaller roughness elements around it to transition.

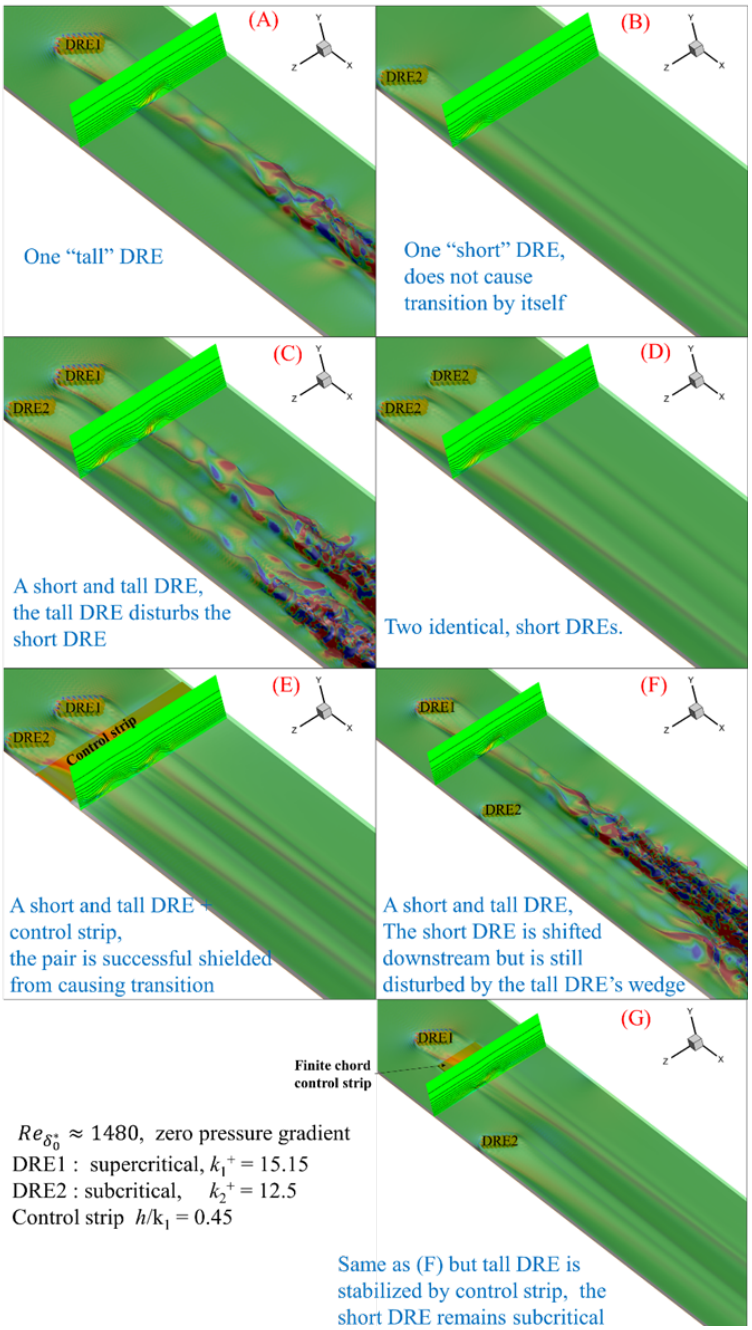

Figure 10. Results on multiple DRE interactions.

Since the mechanisms of transition of a multiple DRE system seem similar to that of an isolated DRE, the same control schemes work: A downstream control strip placed behind the DRE pair (Fig.10E) prevents transition. Also, just suppressing the transition behind the larger DRE (Fig. 10G) can prevent the smaller DRE from transition as the modal disturbances that excite its wake are no longer present. *If we quench the unsteady disturbances soon enough, we may be able to keep them from 'infecting' nearby subcritical wakes.*

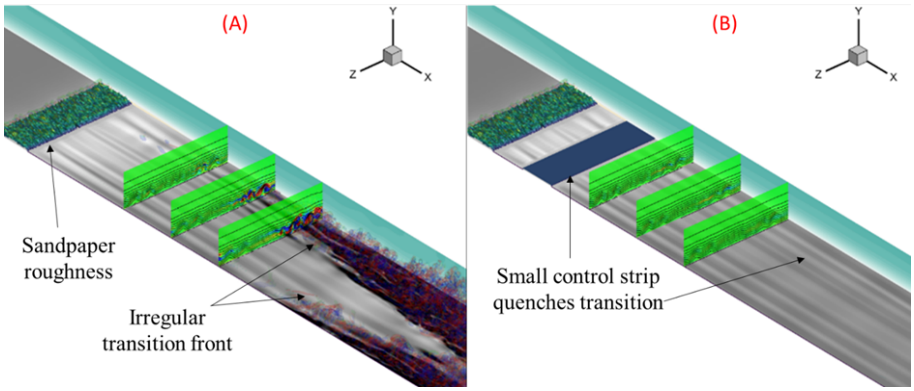

Figure 11. A Transition caused by a sandpaper-like distributed roughness trip. **B.** Mitigation using downstream shielding by a low amplitude control strip.

Additionally, we considered a 'sandpaper' like distributed roughness trip in Fig. 11. Preliminary results show similar mechanisms at play not just in the final stages, but throughout the transition process, at least for this specific distributed roughness considered here, namely (a) generation of streamwise vortices by the interaction of the roughness with the incoming boundary layer, (b) lift-up and transient amplification and (c) that the most dangerous disturbances undergo modal instability, and these may excite subcritical wakes in their neighborhood. Figure 11B shows that shielding strips can delay transition downstream of distributed roughness as well by reducing the magnitude of streamwise vortices, supporting the broad similarity of mechanisms. These results were presented at TSFP12.

We also studied the related problem of the interaction between a turbulent spot and a (subcritical) low-speed streak. For the configurations and parameters considered, the spot is observed to destabilize the streak at a distance, before eventually spreading into it. Like the turbulent wedge, the spot was observed to primarily force the subdominant low-frequency sinuous swaying instability of the streak during the early stage of its destabilization. It was clearly observed that the unsteadiness lasts a lot longer at a given streamwise location when a low-speed streak is present about the spot – the streak continues to remain unstable and generate unsteady streamwise vorticity even after the spot has passed the location. The engineering outcome of this interaction would be a larger intermittency factor and thus a greater overall skin friction and heat transfer than obtained from predictions based on spots evolving in quiescent environments. Results suggest that suppression of spot spreading and reduction of streak amplitude using shielding strips are promising strategies to mitigate this interaction. This work on spots was presented at the ASME-JSME-KSME Fluids Engineering Meeting in 2024 and is set to appear in the special issue of the *Journal of Fluids Engineering*.

(IV) Generality of RIT mechanisms to other modes of transition.

We examined, using a vorticity point of view, late-stage transition mechanisms in roughness induced transition caused by discrete and random distributed roughness, bypass transition caused by strong three-dimensional free stream forcing and a classical transition caused by a large amplitude TS wave interacting with free stream disturbances. Large negative values of $\overline{w'\omega_y'}$ are observed in the late-stage transition in all four cases (Fig. 12). We also found a decrease in wall shear stress when near-wall spanwise motion is suppressed, whereas suppression of spanwise motion far away from the wall does

not immediately alter wall shear stress. This supports the counter-gradient transport of the mean spanwise vorticity by $\overline{w'\omega_y'}$ as the mechanism that increases wall shear stress during transition.

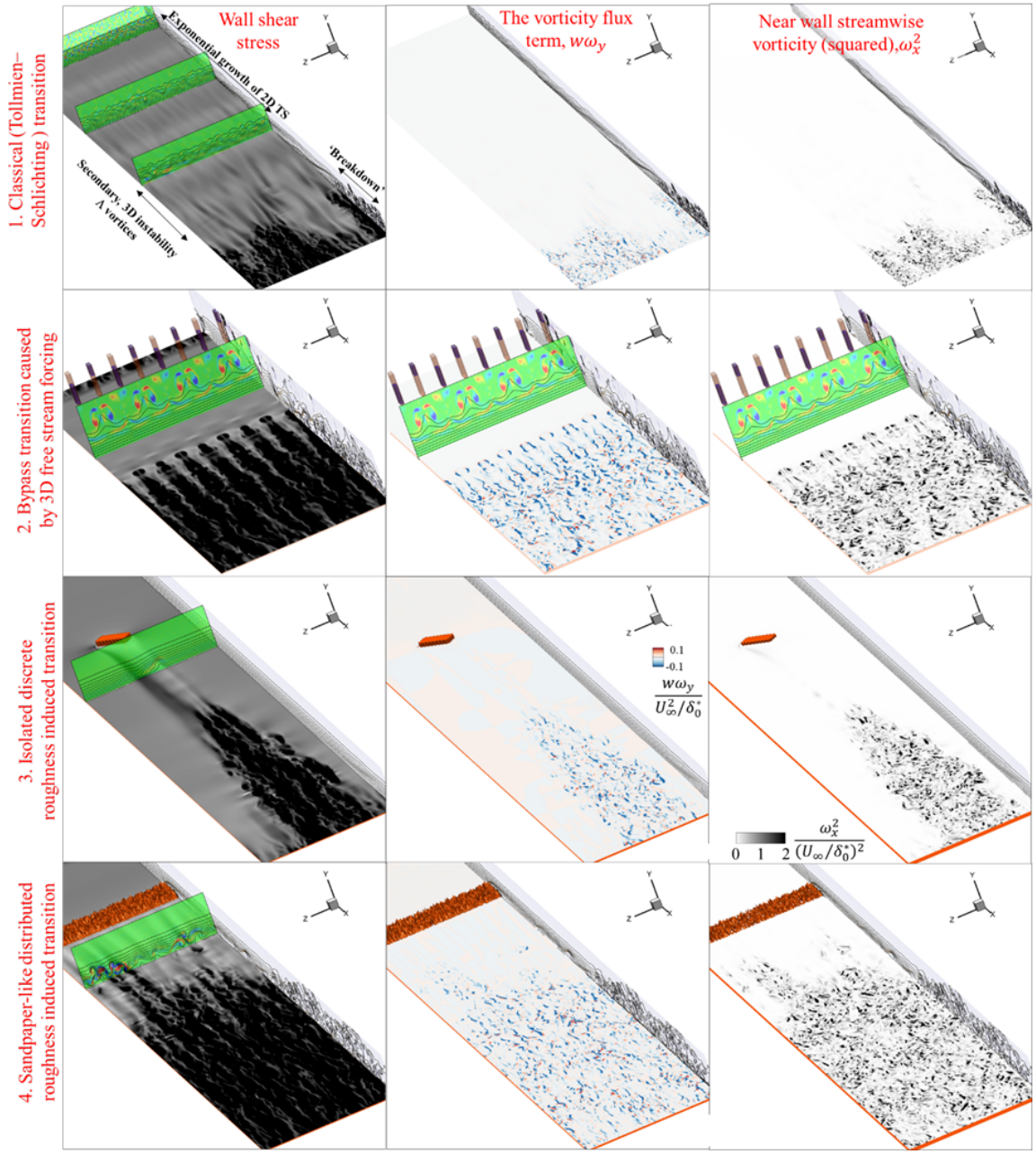

Figure 12. Comparison of boundary layer transition across four different routes.

The underlying mechanism for the increase in wall shear stress during late-stage transition is described below. Positive streamwise vortices (i.e. counterclockwise about the x-axis) would create a negative w below and would lift-up the negative ω_z of sheared flow to create a positive ω_y. Negative streamwise vortices would create a positive w below and a negative ω_y. Either way, the product of w and ω_y will be negative below the streamwise vortex regardless of the sign of that vortex. This mechanism is clearly illustrated in Fig. 13 using a DNS of a steady streamwise vortex in a Couette flow. The streamwise vortex considered here has the strength, core size and height from the wall comparable to a streamwise vortex associated with the various modes of transition. The single (counterclockwise) streamwise vortex induces a positive w above and a negative w below it (Fig. 13A). The magnitude of w is larger below

the vortex due to the image effect to satisfy no through-flow condition at the wall. The streamwise vortex lifts-up spanwise vortex lines to generate positive wall normal vorticity in its neighborhood (Fig. 13B). Thus, the streamwise vortex generates a negative $w\omega_y$ *below* it. This negative $w\omega_y$ causes the high-speed regions near the wall to cover more of the span, thus increasing span-averaged wall shear stress by stretching ω_x near the wall (Fig. 13C). Thus, the mechanism that appears to be universal across the very different transition routes in Fig. 12 can thus be understood by studying a steady, decaying streamwise vortex in Couette flow.

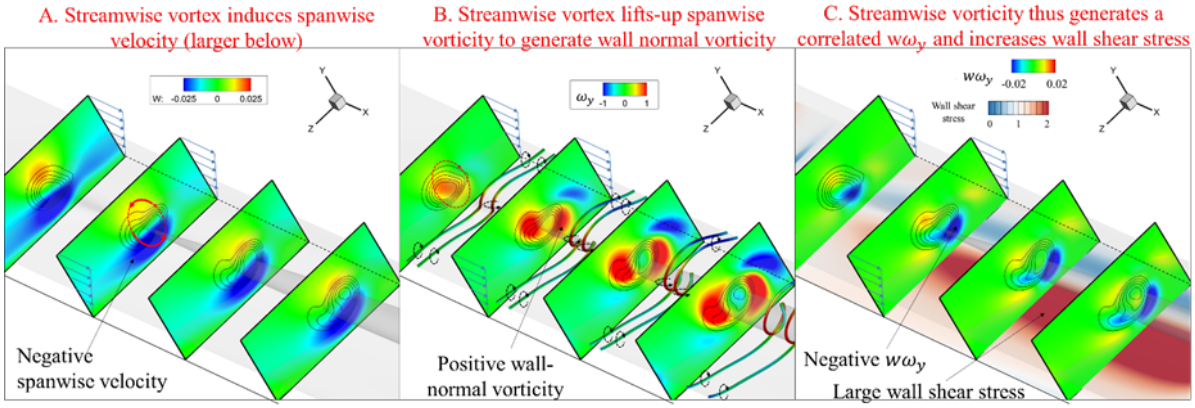

Figure 13: Evolution of a steady (decaying) streamwise vortex in a Couette flow. A. Contours of induced spanwise velocity in cut-planes normal to the streamwise direction; B. ω_y generated by lift-up (along with isosurface of U and vortex lines colored by ω_y); C. $w\omega_y$ and wall shear stress.

Concluding Remarks

This grant has enabled the study of the fundamental mechanisms associated with the interaction of streamwise vortices with shielding strips, the effect of pressure gradients on roughness-induced transition, the generality of late-stage transition, and the interaction of multiple DRE wakes. All these efforts have been achieved using a combination of direct numerical simulations and wind-tunnel experiments. The knowledge generated in this has advanced our understanding of how to mitigate transition on zero-pressure-gradient flat plate boundary layers caused by isolated roughness elements in progressively more challenging and operationally relevant configurations. LSWT experiments which demonstrated shielding over a representative laminar flow airfoil are particularly encouraging in this regard. Ongoing and subsequent work are aimed at the development of refined models and to advance mitigation strategies beyond simple flat strips.

Journal Articles

1. S. Suryanarayanan, D.B. Goldstein, A.R. Berger, E.B. White & G.L. Brown. "Mechanisms of Roughness-Induced Boundary-Layer Transition Control by Shielding, " *AIAA Journal,* Vol. 58, No. 7 (2020), pp. 2951-2963, https://doi.org/10.2514/1.J058950
2. Suryanarayanan, S., Goldstein, D.B., Berger, A.R., White, E.B. and Brown, G.L. "Effect of Pressure Gradients On The Different Stages of Roughness Induced Boundary Layer Transition", 2020, *International Journal of Heat and Fluid Flow*, vol. 86, 108688. https://doi.org/10.1016/j.ijheatfluidflow.2020.108688
3. Suryanarayanan, S., Settlemier, A. and Goldstein, D. "The interaction of turbulent spots with low-speed streaks", *accepted for publication in the Journal of Fluids Engineering*. https://doi.org/10.1115/1.4064852
4. Justiniano E., Brown, L., White, E.B, Suryanarayanan, S. and Goldstein, D.B., "Mitigation of Roughness-Induced Boundary-Layer Transition on Airfoils Using Shielding Strips", *under review, AIAA Journal.*
5. S. Suryanarayanan, D.B. Goldstein & G.L. Brown. "Universal Features In The Final Stages Of Transition To Turbulence In Wall Bounded Flows", *under preparation for submission to Physics of Fluids.*

Conference Publications

1. S. Suryanarayanan, D.B. Goldstein, A.R. Berger, E.B. White & G.L. Brown. "Effect of pressure gradients on the different stages of roughness induced boundary layer transition," *11th International Symposium on Turbulence and Shear Flow Phenomena* (TSFP11), July, 2019, Southampton, UK.
2. Berger, A. R., and E. B. White. "Experimental study of the role of high-and low-speed streaks in turbulent wedge spreading." AIAA Scitech 2020 Forum. Orlando, FL, 6-10 January, 2020. AIAA 2020- 0832. https://doi.org/10.2514/6.2020-0832
3. Suryanarayanan, S., Goldstein, D.B. and Brown G.L., "Interaction of Streamwise Vortices with Surface Textures – DNS and Analysis*". AIAA Aviation* 2020, June 15 – 19, 2020 (Virtual event). AIAA 2020-3020. https://doi.org/10.2514/6.2020-3020
4. Suryanarayanan, S., Goldstein, D., Finke, C., Herrara Hernandez, E., White, E., and Brown, G., "On the evolution of streamwise vortices over solid surfaces: Theory, experiments and matched direct numerical simulations." Scitech 2022. AIAA paper 2022-1196. Published online Dec. 29, 2021. https://doi.org/10.2514/6.2022-1196
5. Suryanarayanan, S., Goldstein, D., White, E. and Brown, G. , "Mechanics of boundary layer transition induced by multiple discrete roughness elements". Paper 398. TSFP12 (Virtual), Osaka, Japan, July 19-22, 2022.
6. E Herrera Hernandez, W Matthews, E Justiniano, EB White, DB Goldstein, and S.Suryanarayanan, "Experiments on Streamwise Vortex Mitigation Using Two-Dimensional Shielding Strips", AIAA SCITECH 2023 Forum, National Harbor, MD & Online, January 23-27, 2023. AIAA 2023-0099 (https://doi.org/10.2514/6.2023-0099).
7. Justiniano, E., Brown, L., White, E., Suryanarayanan, S., Goldstein, D., 2023. "Mitigation of airfoil boundary -layer transition due to leading edge roughness using shielding strips.", AIAA AVIATION 2023 Forum, 12-16 June 2023, San Diego, CA and Online. AIAA 2023-3998. (https://doi.org/10.2514/6.2023-3998)

Talks

1. S. Suryanarayanan, D.B. Goldstein, A.R. Berger, E.B. White & G.L. Brown. "Effect Of Pressure Gradients On The Different Stages Of Roughness Induced Boundary Layer Transition", Presented at *The Eleventh International Symposium on Turbulence and Shear Flow Phenomena* (TSFP11), July 30 to August 2, 2019, Grand Harbour Hotel, Southampton, UK.
2. D.B. Goldstein, S. Suryanarayanan, & G.L. Brown. "On the final stages of transition to turbulence in wall bounded flows", presented at *71st Annual Meeting of the American Physical Society's Division of Fluid Dynamics* (DFD), November 18-20, 2018, Atlanta, Georgia.
3. S. Suryanarayanan, D.B. Goldstein, A.R. Berger, E.B. White & G.L. Brown. "Role of flow acceleration on the vorticity dynamics of roughness induced transition," Bluebonnet Symposium, SMU, May, 2019.
4. S. Suryanarayanan, D.B. Goldstein, and Brown, G., 2019. `` Some Universal Features in the Final Stages of Transition to Turbulence in Wall Bounded Flows." Poster presented at IUTAM Symposium on Laminar-Turbulent Transition, September 2-6, 2019, London, UK.
5. Suryanarayanan, S., Goldstein, D.B. and Brown, G.L, "On the interaction of streamwise vortices with surface textures", talk given by Suryanarayanan at the *72nd Annual Meeting of the APS Division of Fluid Dynamics*, Seattle WA, November 23-26, 2019.
6. Suryanarayanan, S., Goldstein, D.B., White, E.B. and Brown, G.L., "Interaction of Streamwise Vortices with Surface Textures: Effects of Differential Flow Displacement and Acceleration", talk given by Suryanarayanan at the *73nd Annual Meeting of the APS Division of Fluid Dynamics*, November 22-24, 2020 (Virtual event).
7. Tusa, C., Suryanarayanan, S., Goldstein, D.B., Justiniano, E. and White, E.B.., "Roughness induced transition on boundary layers with realistic pressure distributions", talk given by Tusa at the *73nd Annual Meeting of the APS Division of Fluid Dynamics*, November 22-24, 2020 (Virtual event).
8. Tusa, C., Suryanarayanan, S., Goldstein, D.B., Justiniano, E. and White, E.B.., "Matched DNS and experiments of roughness induced transition over realistic airfoil", talk given by Tusa at the *74th Annual Meeting of the APS Division of Fluid Dynamics*, November 21-23, 2021.
9. Suryanarayanan, S., Settlemier, A., Goldstein, D. 2023. The interaction of turbulent spots with low-speed streaks. Talk given by Suryanarayanan at the ASME-JSME-KSME Joint Fluids Engineering Conf. Osaka, July 9-13, 2023.
10. Invited Lecture, given by Goldstein: The Oden Institute, (UT Austin), Nov. 9, 2021
11. Invited Lecture, given by Suryanarayanan : The Indian Institute of Science, January 12, 2023.
12. Invited Lecture, given by Goldstein: Rensselaer Polytechnic Institute, March 1, 2023

Students supported in whole or in part: Charles Tusa (MS) currently at Siemens Digital Industries Software, Colton Finke (M.S.) currently at Lockheed-Martin, Eleazar Hererra (M.Eng. pending) currently at Blue Origin, Ezequiel Justiniano (Ph.D.) currently at Sky Loom (inter-satellite laser communications development).

Postdoc/Research Associates supported in whole or in part: Saikishan Suryanarayanan (at UT Austin till August 2022), currently a tenure-track Assistant Professor at the University of Akron.

Faculty supported in part: David Goldstein, Edward White, Garry Brown